Altered pre-lamin A processing is a common mechanism leading to lipodystrophy

Cristina Capanni[1], Elisabetta Mattioli[2], Marta Columbaro[2], Enrico Lucarelli[3], Veena K. Parnaik[4], Giuseppe Novelli[5], Manfred Wehnert[6], Vittoria Cenni[2], Nadir M. Maraldi[1,2], Stefano Squarzoni[1] and Giovanna Lattanzi[1,*]

[1]ITOI, CNR, Unit of Bologna, c/o IOR, Bologna, Italy, [2]Laboratory of Cell Biology, Istituti Ortopedici Rizzoli, Bologna, Italy, [3]Regeneration and Tissue Engineering Laboratory of the Musculoskeletal Tissue Bank, IOR, Bologna, Italy, [4]Centre for Cellular and Molecular Biology, Hyderabad 500 007, India, [5]Department of Biopathology and Image Diagnostics, University of Rome Tor Vergata, Rome, Italy and [6]Institute of Human Genetics, University of Greifswald, Germany

Lipodystrophies are a heterogeneous group of human disorders characterized by the anomalous distribution of body fat associated with insulin resistance and altered lipid metabolism. The pathogenetic mechanism of inherited lipodystrophies is not yet clear; at the molecular level they have been linked to mutations of lamin A/C, peroxisome proliferator-activated receptor (PPARγ) and other seemingly unrelated proteins. In this study, we examined lamin A/C processing in three laminopathies characterized by lipodystrophic pheno-types: Dunnigan type familial partial lipodystrophy, mandibuloacral dysplasia and atypical Werner's syndrome. We found that the lamin A precursor was specifically accumulated in lipodystrophy cells. Pre-lamin A was located at the nuclear envelope and co-localized with the adipocyte transcription factor sterol regulatory element binding protein 1 (SREBP1). Using co-immunoprecipitation experiments, we obtained the first demonstration of an *in vivo* interaction between SREBP1 and pre-lamin A. Binding of SREBP1 to the lamin A precursor was detected in patient fibroblasts as well as in control fibroblasts forced to accumulate pre-lamin A by farnesylation inhibitors. In contrast, SREBP1 did not interact *in vivo* with mature lamin A or C in cultured fibroblasts. To gain insights into the effect of pre-lamin A accumulation in adipose tissue, we inhibited lamin A precursor processing in 3T3-L1 pre-adipocytes. Our results show that pre-lamin A seques-ters SREBP1 at the nuclear rim, thus decreasing the pool of active SREBP1 that normally activates PPARγ and causing impairment of pre-adipocyte differentiation. This defect can be rescued by treatment with trogli-tazone, a known PPARγ ligand activating the adipogenic program.

INTRODUCTION

Lipodystrophies are a heterogeneous group of human dis-orders characterized by the anomalous distribution of body fat or generalized loss of adipose tissue (1). Various degrees of insulin resistance are associated with these diseases. Several types of lipodystrophy have been characterized at the molecular genetic level, including Dunnigan-type familial partial lipodystrophy (FPLD) (2), partial lipodystrophy with mandibuloacral dysplasia (MAD) (3), syndromes of partial lipodystrophy with cardiomyopathy (4) and Berardinelli–Seip

congenital generalized lipodystrophy (5). In FPLD and MAD, lamin A/C mutations have been linked to disease (2,3), whereas a form of partial lipodystrophy associated with PPARγ mutations has also been described (6). Berardi-nelli–Seip congenital generalized lipodystrophy is due to mutations of seipin, an endoplasmic reticulum protein (5). Other lipodystrophies are acquired or drug-induced, such as the lipodystrophy syndrome that is associated with the use of highly active antiretroviral treatment (HAART) (7) (reviewed in 1). In addition, progeroid syndromes such as Hutchinson–Gilford progeria (HGPS) and atypical Werner's

*To whom correspondence should be addressed at: ITOI, CNR, Unit of Bologna, c/o IOR, Via di Barbiano 1/10, I-40136 Bologna, Italy. Tel: +39 0516366768; Fax: +39 051583593; Email: lattanzi@jolly.bo.cnr.it

syndrome (WS) show generalized lipodystrophy, often combined with insulin resistant diabetes mellitus (8–11).

In recent years, two major players have emerged as being possibly involved in the pathogenesis of lipodystrophies. The first is lamin A/C, the nuclear lamina constituent mutated in FPLD and MAD cells (2,3) as well as in progeroid syndromes with lipodystrophy (8–11). Moreover, mutations of ZMPSTE 24, the metalloprotease involved in lamin A processing (12), cause diseases featuring a lipodystrophy phenotype such as MAD in humans (13), a MAD-resembling phenotype in knockout mice (14,15) and a HGPS (Markquardt, personal communication).

The second emerging protein in the pathogenesis of lipodystrophy is the sterol regulatory element binding protein 1 (SREBP1), a transcription factor whose localization and trans-activation ability appear to be altered in acquired lipodystrophy (7,16). In this context, it is noteworthy that mutations of PPARγ transcription factor, which is transcribed downstream of SREBP1 activation and mediates adipocyte differentiation (17), are responsible for other forms of partial lipodystrophy (6,18). Moreover, a single point mutation in the PPARγ promoter has been recently associated with FPLD (19).

Lamins A and C are nuclear lamina proteins obtained by alternative splicing of *LMNA* and are almost ubiquitously expressed in differentiated tissues (20). Before being assembled in the nuclear lamina, lamin A undergoes complex post-translational modifications including farnesylation of the C-terminus and protease cleavage (12,13,21). Farnesylation of pre-lamin A is necessary for the following steps of protein cleavage, as metalloproteases fail to bind non-farnesylated lamin A sequence (15). Mature lamin A forms a heterodimeric complex with lamin C (22), which appears to play structural and functional roles, not completely elucidated (20). Lamin A/C interacts with lamin B and emerin (23) as well as constituents of the nuclear matrix including lamina-associated polypeptide (LAP) 2 alpha (24), nuclear actin (25,26), transcription factor E2F and protein Rb (27). An increasing number of *LMNA* mutations give rise to several diseases grouped under the definition of laminopathies, but characterized by different tissue-specific defects (28). Besides the earlier-mentioned disorders affecting adipose tissue and/or causing pre-mature aging, *LMNA*-linked disorders include autosomal-dominant Emery–Dreifuss muscular dystrophy (EDMD) (29), limb-girdle muscular dystrophy type 1B (30), dilated cardiomyopathy with conduction system disease (31) affecting skeletal and/or cardiac muscle and other diseases affecting different tissues such as Charcot–Marie–Tooth neuropathy type 2 (32). The pathogenesis of EDMD and other laminopathies has been extensively investigated in recent years (33–37) and there is circumstantial evidence that lamin A/C interaction with either nuclear envelope constituents or chromatin may be affected in the diseases (20,38–42).

SREBP/ADD1 was initially cloned from rat adipose tissue (43) and shown to be activated in cultured fibroblasts, adipocytes and liver (44,45). The human homolog of ADD1, SREBP1, plays a major role in the control of genes involved in adipocyte differentiation, whereas a closely related factor, SREBP2, is mostly related to cholesterol metabolism (46). SREBP1 is synthesized as an 125 kDa precursor and it is embedded in the endoplasmic reticulum membrane. Depletion of cholesterol causes proteolytic cleavage of the transcriptionally active N-terminal portion of SREBP1 from its position to allow translocation into the nucleus (47). A number of published data suggest that SREBP1 interacts with the nuclear envelope at an undefined site, while being transferred from the endoplasmic reticulum to the nuclear interior (48). Interestingly, SREBP1 and lamin A/C do interact *in vitro* (34), suggesting that alteration of their interplay may underlie the pathogenic mechanism of lipodystrophies. Recent evidence shows that impairment of SREBP1 accumulation inside the nucleus occurs in pre-adipocytes treated with an agent employed in HAART and causative of acquired lipodystrophy (7,16). Retention of SREBP1 at the nuclear envelope is observed under these experimental conditions, concomitant with anomalous accumulation of unprocessed lamin A at the nuclear rim (7). Downstream of SREBP1 retention at the nuclear envelope, activation of the transcription factor PPARγ, which regulates adipocyte differentiation, is impaired (16), indicating a possible pathogenetic pathway for acquired lipodystrophy.

In this study, we evaluated lamin A precursor maturation and intermolecular interactions in *LMNA*-mutated FPLD, MAD and WS fibroblasts and control fibroblasts. Our results show that pre-lamin A is processed to a reduced rate in FPLD, MAD and WS cells leading to precursor protein accumulation. Pre-lamin A is bound to SREBP1 at the nuclear rim, thus limiting translocation of the transcription factor to the nuclear interior. By using 3T3-L1 pre-adipocytes as a cellular model, we also show that forced pre-lamin A accumulation reduces the rate of DNA-bound SREBP1 and lowers PPARγ expression. The downstream effects of reduced PPARγ expression can be rescued by troglitazone (TZD) treatment.

RESULTS

Pre-lamin A accumulates in FPLD, MAD and WS fibroblasts

A faint pre-lamin A band was detected in control skin fibroblasts by western blot analysis (Fig. 1A). The amount of lamin A precursor was increased in MAD, FPLD and WS fibroblasts when compared with controls (wild-type or EDMD2 fibroblasts) (Fig. 1A), whereas lamin A/C and emerin amounts were not significantly changed (Fig. 1A). Quantitative analysis showed a statistically significant increase in pre-lamin A amount in MAD, FPLD and WS fibroblasts when compared with control fibroblasts (Fig. 1B). Immunofluorescence labeling of pre-lamin A showed an intense nuclear rim staining in MAD, FPLD and WS fibroblasts (Fig. 1C), whereas the precursor protein was hardly detectable in wild-type cells (Fig. 1C). Moreover, a faint pre-lamin A staining was detected at the nuclear rim of R401C-mutated EDMD2 cells (Fig. 1C) and in other EDMD2 cell lines bearing five different *LMNA* mutations (data not shown). Intra-nuclear pre-lamin A-labeled structures were observed in MAD, FPLD and WS fibroblasts (Fig. 1C, arrowheads). Mis-localization of pre-lamin A to intra-nuclear structures was observed in a percentage of EDMD2 cells (Fig. 1C) (data not shown). Emerin co-localized with pre-lamin A at the nuclear rim, whereas pre-lamin A-labeled
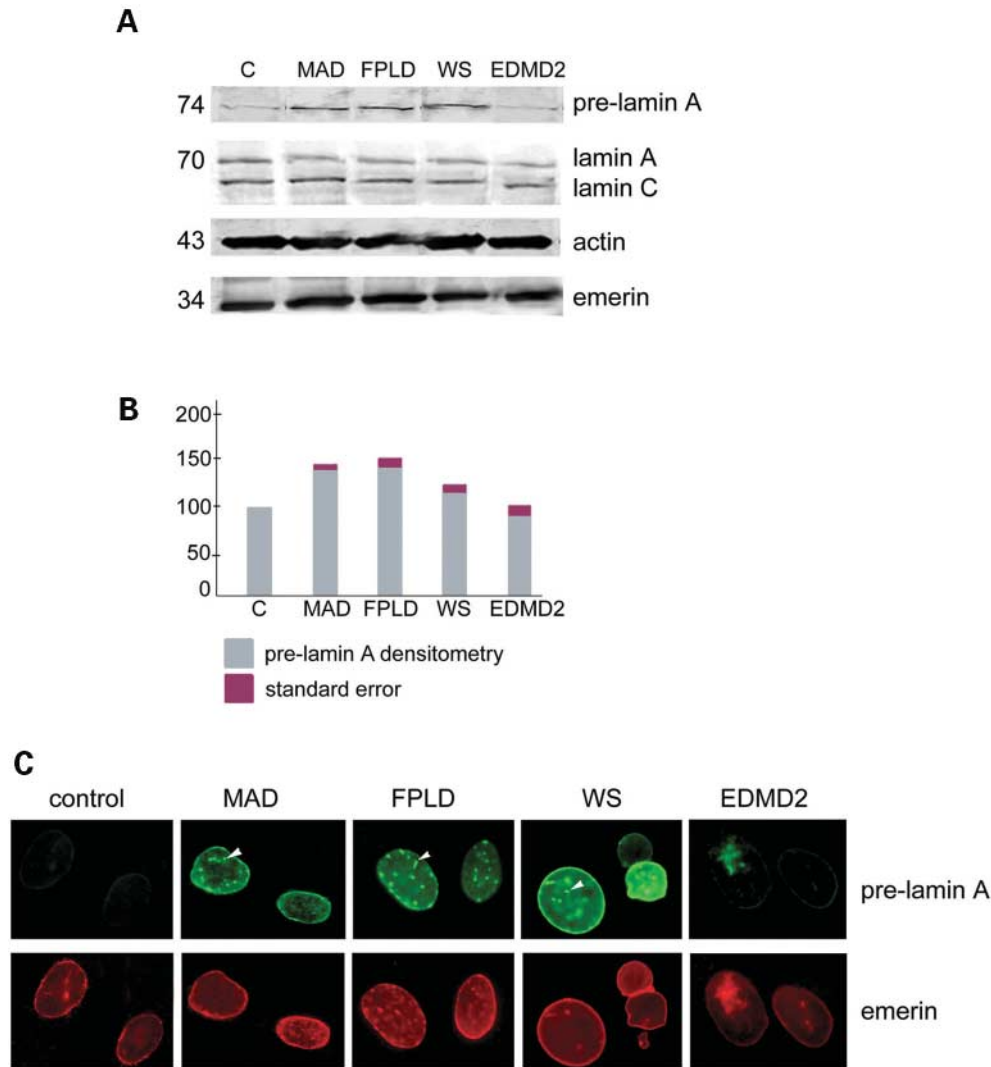
Figure 1. Analysis of pre-lamin A expression and localization in control and laminopathic fibroblasts. **(A)** Western blot analysis of pre-lamin A in untreated skin fibroblasts. Whole cell lysates from control (C), MAD, FPLD, WS and EDMD2 fibroblasts were submitted to electrophoresis, western blotted and probed using anti-pre-lamin A antibody. Immunoblotted membranes were stripped and re-probed with anti-lamin A/C, anti-emerin or anti-actin antibodies (lower panels). Actin staining shows equal loading of samples. Molecular weight markers are reported in kilodalton. **(B)** Densitometric analysis of pre-lamin A immunoblotted bands shown in panel (A). Immunoblotted bands were quantified by densitometry. At least three independent experiments were performed for western immunoblot analysis of pre-lamin A accumulation, equal loading of samples was checked using actin as an internal loading control and data were calculated as percentage of control pre-lamin A densitometry obtained in each experiment. Values are reported as a percentage of control pre-lamin A amount (mean $\pm$ SEM of three different experiments). Densitometric values obtained for untreated MAD, FPLD and WS samples are significantly different from control values, as calculated by Student's *t*-test ($P < 0.05$). **(C)** Localization of pre-lamin A in control, MAD, FPLD, WS and EDMD2 fibroblasts. Double-staining of pre-lamin A and emerin was performed by anti-pre-lamin A polyclonal antibody (Santa Cruz, SC-6214, revealed by FITC-conjugated secondary antibody) and anti-emerin monoclonal antibody (revealed by Cy-3-conjugated secondary antibody). Pictures were obtained by fluorescence microscopy. Pre-lamin A-labeled intra-nuclear structures are marked by arrowheads.

intra-nuclear structures did not co-localize with emerin in lipodystrophy nuclei (Fig. 1C).

To check whether farnesylation of lamin A precursor was an ongoing process in the examined cell lines, we performed mevinolin treatment (21). Accumulation of unprocessed lamin A was observed after mevinolin treatment in all examined cell lines (compare Fig. 2A with Fig. 1A), but a higher pre-lamin A amount was detected in FPLD, MAD and WS fibroblasts by western immunoblot (compare Fig. 2A with Fig. 1A). Mature lamin A band was slightly reduced in mevinolin-treated samples, whereas lamin C and emerin expressions were not or slightly affected by mevinolin

administration (compare Fig. 2A with Fig. 1A). Densitometric analysis of pre-lamin A immunoblotted bands showed an increase in each mevinolin-treated control and laminopathic cell line when compared with its corresponding untreated cell line (Fig. 2B). In wild-type fibroblasts forced to accumulate pre-lamin A, nuclear lamina invaginations were observed (Fig. 2C and C′, arrowheads): pre-lamin A-labeled structures were detected in the equatorial plane of the nucleus (Fig. 2C′), starting from the nuclear rim (Fig. 2C′). Nuclear lamina invaginations were also observed in MAD and WS fibroblasts (Fig. 2C, arrowheads), whereas FPLD nuclei showed anomalous pre-lamin A aggregates localized at the
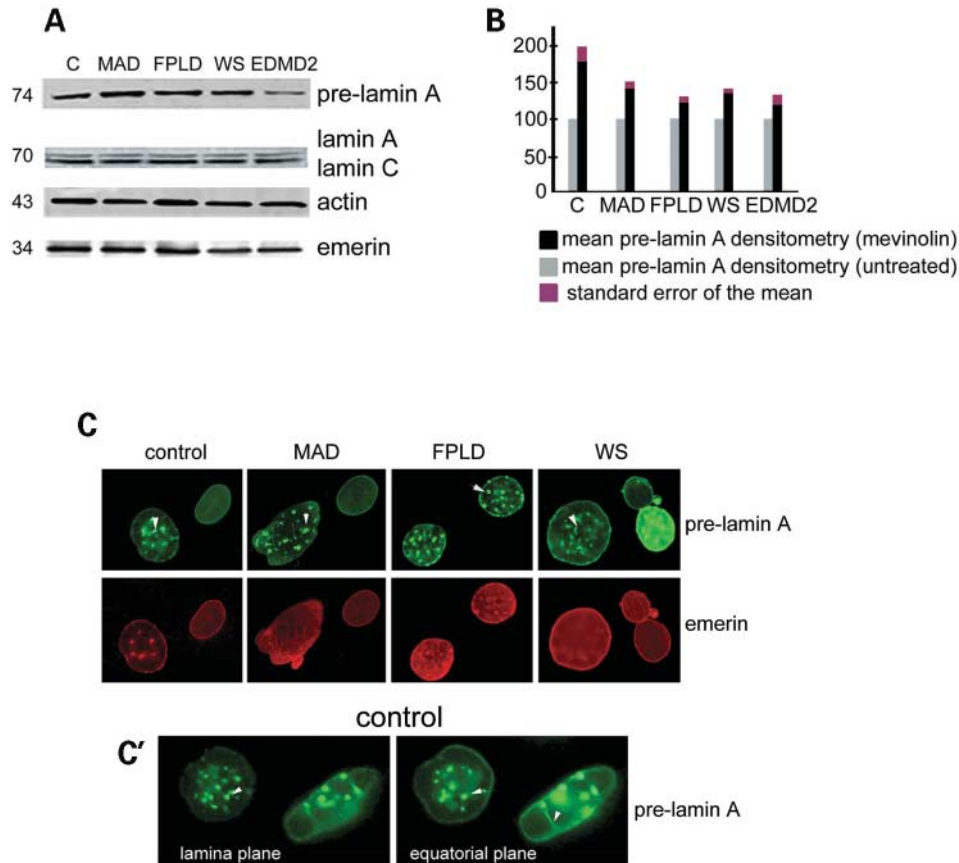
Figure 2. Analysis of pre-lamin A expression and localization in mevinolin-treated control and laminopathic fibroblasts. **(A)** Western blot analysis of pre-lamin A in skin fibroblasts, following 18 h mevinolin treatment. Whole cell lysates from control (C), MAD, FPLD, WS and EDMD2 fibroblasts were submitted to electrophoresis, western blotted and probed using anti-pre-lamin A antibody. Immunoblotted membranes were stripped and re-probed with anti-lamin A/C, anti-emerin or anti-actin antibodies (lower panels). Actin staining shows equal loading of samples. Molecular weight markers are reported in kilodaltons. **(B)** Densitometric analysis of pre-lamin A immunoblotted bands shown in panel (A). Immunoblotted bands were quantified by densitometry. At least three independent experiments were performed for western immunoblot analysis of pre-lamin A accumulation. Equal loading of samples was checked using actin as an internal loading control and data were calculated as percentage of pre-lamin A densitometry measured in each untreated cell line. Values are reported as a percentage of pre-lamin A amount in each corresponding untreated cell line (Fig. 1A and B) and they represent means $\pm$ SEM of three different experiments. Western blotting of untreated fibroblasts (Fig. 1A) and mevinolin-treated fibroblasts (A) was routinely performed on the same membrane to allow comparison of results. **(C)** Localization of pre-lamin A in mevinolin-treated control, MAD, FPLD and WS fibroblasts. Double-staining of pre-lamin A and emerin was performed by anti-pre-lamin A polyclonal antibody (Santa Cruz, SC-6214, revealed by FITC-conjugated secondary antibody) and anti-emerin monoclonal antibody (revealed by Cy-3-conjugated secondary antibody **(C′)** Localization of pre-lamin A in mevinolin-treated wild-type nuclei (control). Pictures were obtained at two different focal planes (lamina plane, equatorial plane). Pre-lamin A-labeled intra-nuclear structures shown in (C) and (C′) are marked by arrowheads. Pictures were obtained by fluorescence microscopy.

nuclear rim (Fig. 2C) (data not shown) (42). In mevinolin-treated wild-type fibroblasts, pre-lamin A-labeled intra-nuclear structures partially co-localized with emerin, whereas they did not co-localize with emerin in MAD, FPLD or WS nuclei (Fig. 2C).

SREBP1 is bound to pre-lamin A *in vivo*

SREBP1 was detected in control and laminopathic fibroblasts as an 125 kDa precursor and as an active cleaved form (68 kDa) (Fig. 3A). An additional low molecular weight band was observed in mevinolin-treated controls and in FPLD, MAD and WS fibroblasts (Fig. 3A). *In vivo* binding of pre-lamin A to the active 68 kDa SREBP1 form was detected in control human fibroblasts following mevinolin-treatment (Fig. 3A) and in FPLD, MAD and WS fibroblasts either untreated (Fig. 3A) or after mevinolin administration (data

not shown). Co-precipitation of SREBP1 and pre-lamin A was observed using either anti-pre-lamin A or anti-SREBP1 antibody to immunoprecipitate protein complexes (Fig. 3A). In contrast, we failed to co-immunoprecipitate lamin A/C using anti-SREBP1 antibody (Fig. 3A). Moreover, lamin A/C was not co-precipitated by anti-pre-lamin A antibody (Fig. 3A). An emerin immunoprecipitation was performed as a control, which showed absence of co-precipitation of SREBP1 (Fig. 3A). These results were confirmed by immuno-precipitation experiments using anti-lamin A/C antibody (Fig. 3B). SREBP1 was not detected in the protein complex precipitated by anti-lamin A/C antibody (Fig. 3B). It should be noted that only in fibroblasts expressing high pre-lamin A levels, cross-reactivity of anti-lamin A/C antibody with pre-lamin A caused immunoprecipitation of pre-lamin A (and co-precipitation of a proportional amount of SREBP1) by
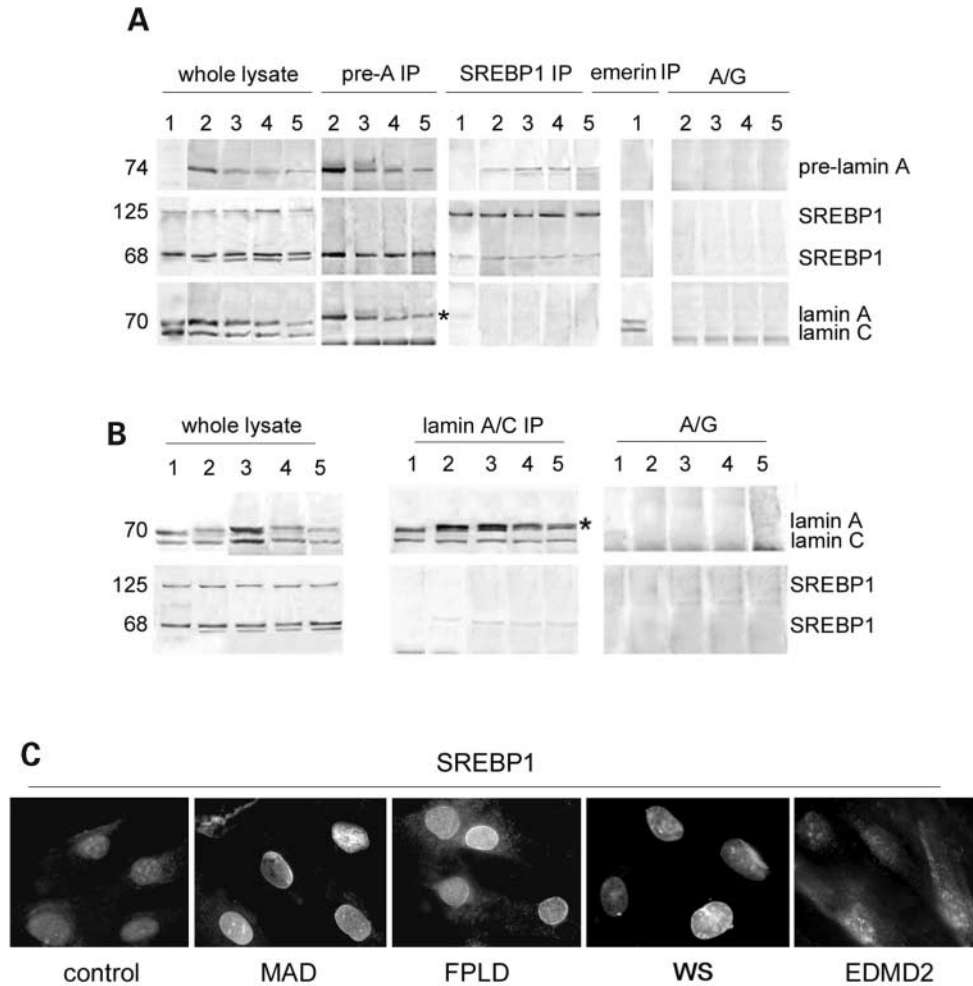
Figure 3. Detection of SREBP1–pre-lamin A binding in human fibroblasts. **(A)**. Western blot analysis of whole lysates from control (lane 1), mevinolin-treated control (lane 2), MAD (lane 3), FPLD (lane 4) and WS fibroblasts (lane 5) is shown in the left panel (whole lysate). Untreated or mevinolin-treated control fibroblasts and untreated FPLD, MAD and WS fibroblast lysates were subjected to immunoprecipitation using anti-pre-lamin A (pre-A IP) or anti-SREBP1 antibody (SREBP1 IP). Co-immunoprecipitated proteins were separated by electrophoresis, western blotted and probed with anti-pre-lamin A and anti-SREBP1 and anti-lamin A/C antibodies. Anti-emerin antibody was used to immunoprecipitate protein complexes, as a specificity control (emerin IP). Active SREBP1 is detected as a 68 kDa band, the uncleaved protein as an 125 kDa band. An additional SREBP1 band below 68 kDa is observed in cellular lysates accumulating pre-lamin A. **(B)** Untreated (lane 1) or mevinolin-treated (lane 2) control fibroblasts and untreated MAD (lane 3), FPLD (lane 4) and WS fibroblast lysates (lane 5) were subjected to immunoprecipitation using anti-lamin A/C antibody (lamin A/C IP). Co-immunoprecipitated proteins were separated by electrophoresis, western blotted and probed with anti-lamin A/C and anti-SREBP1 antibody. Protein A/G panels (A/G) show the absence of non-specific binding when primary antibody is omitted in the immunoprecipitation mixture. Asterisks in panel A and B mark pre-lamin A band detected by anti-lamin A/C antibody. Molecular weight markers are reported in kilodaltons. **(C)** Localization of SREBP1 in wild-type, MAD, FPLD, WS and EDMD2 fibroblasts. SREBP1 is labeled by anti-SREBP1 antibody and it is detected by FITC-conjugated secondary antibody. Pictures are obtained by fluorescence microscopy.

anti-lamin A/C antibody (Fig. 3B). Figure 3C shows immuno-fluorescence labeling of SREBP1 in wild-type, MAD, FPLD, WS and EDMD2 fibroblasts. The transcription factor was localized inside the nucleus of control fibroblasts (wild-type and R401C EDMD2 fibroblasts) and a faint cytoplasmic labeling was observed (Fig. 3C). In MAD, FPLD and WS fibroblasts, nuclear rim staining was also observed (Fig. 3C).

Pre-lamin A accumulation in 3T3-L1 pre-adipocytes causes SREBP1 retention at the nuclear rim

In differentiating 3T3-L1 pre-adipocytes, a sharp SREBP1 68 kDa band was detected by western blot analysis, while the 125 kDa precursor protein was less intensely stained

(Fig. 4A). Mevinolin treatment caused accumulation of pre-lamin A, whereas SREBP1 level was not affected (Fig. 4A, lanes 1 and 2).

A stable interaction between SREBP1 and pre-lamin A was detected by co-immunoprecipitation assay in differentiating 3T3-L1 adipocytes induced to accumulate unprocessed lamin A (Fig. 4A). This result was obtained using either anti-pre-lamin A or anti-SREBP1 antibody to co-precipitate protein complexes (Fig. 4A, lanes 3–6). Even in differentiating 3T3-L1 adipocytes, we failed to detect SREBP1-lamin A/C binding (Fig. 4A, lanes 3–8).

To investigate the role of SREBP1–pre-lamin A interaction, we first checked the sub-cellular distribution of SREBP1 in 3T3-L1 pre-adipocytes, accumulating or not pre-lamin
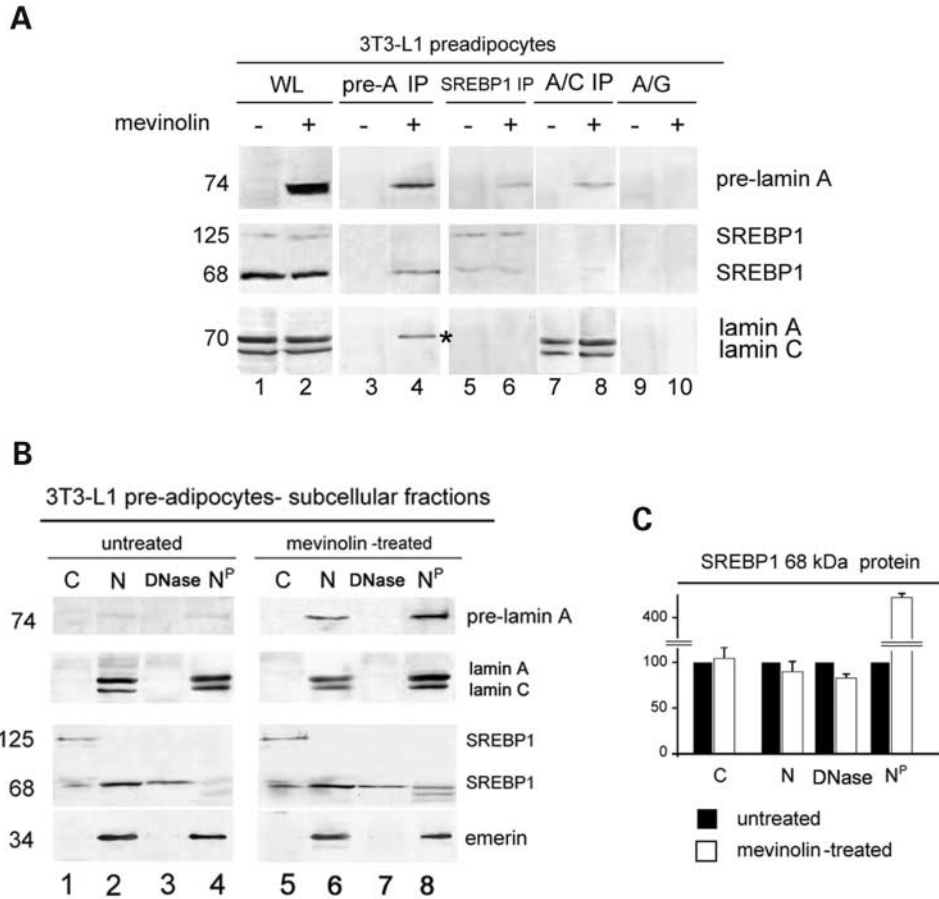
A

3T3-L1 preadipocytes

	WL	pre-A IP	SREBP1 IP	A/C IP	A/G
mevinolin	− +	− +	− +	− +	− +

74 ————————————————— pre-lamin A

125 ————————————————— SREBP1
68 ————————————————— SREBP1

70 ———————————————— lamin A / lamin C

1 2   3 4   5 6   7 8   9 10

B

3T3-L1 pre-adipocytes- subcellular fractions

	untreated	mevinolin -treated
	C N DNase N^P	C N DNase N^P

74 ———————————————— pre-lamin A

———————————————— lamin A / lamin C

125 ———————————————— SREBP1

68 ———————————————— SREBP1

34 ———————————————— emerin

1 2 3 4   5 6 7 8

C

SREBP1 68 kDa protein

400

100

50

0

C   N   DNase   N^P

■ untreated
□ mevinolin-treated

Figure 4. SREBP1–pre-lamin A interaction in 3T3-L1 pre-adipocytes. **(A)** Detection of SREBP1–pre-lamin A binding in 3T3-L1 pre-adipocytes. Cellular lysates from 3T3-L1 cells (treated or not with mevinolin) were subjected to immunoprecipitation using anti-pre-lamin A (pre-A IP, lanes 3 and 4), anti-SREBP1 (SREBP1 IP, lanes 5 and 6) or anti-lamin A/C antibody (A/C IP, lanes 7 and 8). Co-precipitated proteins were separated by electrophoresis, western blotted and probed with anti-pre-lamin A and anti-SREBP1 antibodies. Western blot analysis of the whole cellular lysate (WL) used as input is shown in lanes 1 and 2. Active SREBP1 is detected as a 68 kDa band, the uncleaved protein as an 125 kDa band (middle). Stripped membranes were re-probed with anti-lamin A/C antibody. Asterisk in the lower panel shows pre-lamin A band detected by anti-lamin A/C antibody. Protein A/G panel (A/G) shows the absence of non-specific binding when primary antibody is omitted in the immunoprecipitation mixture (lanes 9 and 10). Molecular weight markers are reported in kilodaltons. **(B)** Biochemical analysis of the sub-cellular distribution of SREBP1 and pre-lamin A in untreated or mevinolin-treated 3T3-L1 pre-adipocytes. Cell pellets were resuspended in a lysis buffer containing 10 mM Tris pH 7.8, 1% NP-40, 10 mM 2-mercaptoethanol and protease inhibitors. Separation of nuclei (N) was obtained by hypotonic shock and shearing: DNase extraction of nuclei was performed using 100 U/ml of DNase; soluble fraction (DNase) and nuclear matrix proteins (N^P) were separated by centrifugation. Each sub-cellular fraction was resuspended in sample buffer, subjected to electrophoresis and western blot and probed with anti-pre-lamin A and anti-SREBP1 antibodies. Stripped membranes were re-probed with anti-emerin antibody as a loading control. Lanes 1 and 5 represent cytosolic fractions (C); lanes 2 and 6 represent purified nuclei (N); lanes 3 and 7 represent DNase soluble nuclear fractions (DNase) and lanes 4 and 8 represent insoluble nuclear fractions (N^P). Molecular weight markers are reported in kilodaltons. **(C)** Densitometric analysis of 68 kDa SREBP1 immunoblotted bands shown in panel (B). Immunoblotted bands were quantified by densitometry. Values are reported as a percentage of 68 kDa SREBP1 band detected in each corresponding untreated adipocyte fraction (mean ± SEM of three different experiments). Western blotting of untreated fibroblast fractions (B, untreated) and mevinolin-treated fibroblast fractions (B, mevinolin-treated) was routinely performed on the same membrane to allow comparison of results.

A. Faint SREBP1 bands were detected in the cytoplasmic fractions (Fig. 4B, lanes 1 and 5), whereas the 68 kDa cleaved protein only was recovered in the nuclear fractions (Fig. 4B, lanes 2–4 and 6–8). In untreated nuclei, the 68 kDa active SREBP1 form was almost completely solubilized after DNase treatment (Fig. 4B, lane 3), whereas SREBP1 band was hardly detectable in the insoluble nuclear fraction (Fig. 4B, lane 4). In contrast, in mevinolin-treated nuclei, active SREBP1 band was clearly detected both in the DNase soluble fraction (Fig. 4B, lane 7) and in the insoluble nuclear fraction (Fig. 4B, lane 8). As expected, pre-lamin A was recovered in purified nuclei from mevinolin-treated cells

(Fig. 4B, lane 6) and it was almost completely retained in the insoluble nuclear fraction after DNase extraction (Fig. 4B, lane 8). Densitometric analysis showed that the amount of activated SREBP1 recovered in the insoluble nuclear fraction was significantly increased in 3T3-L1 pre-adipocytes accumulating pre-lamin A (Fig. 4C).

SREBP1 is retained at the nuclear rim of cells accumulating pre-lamin A

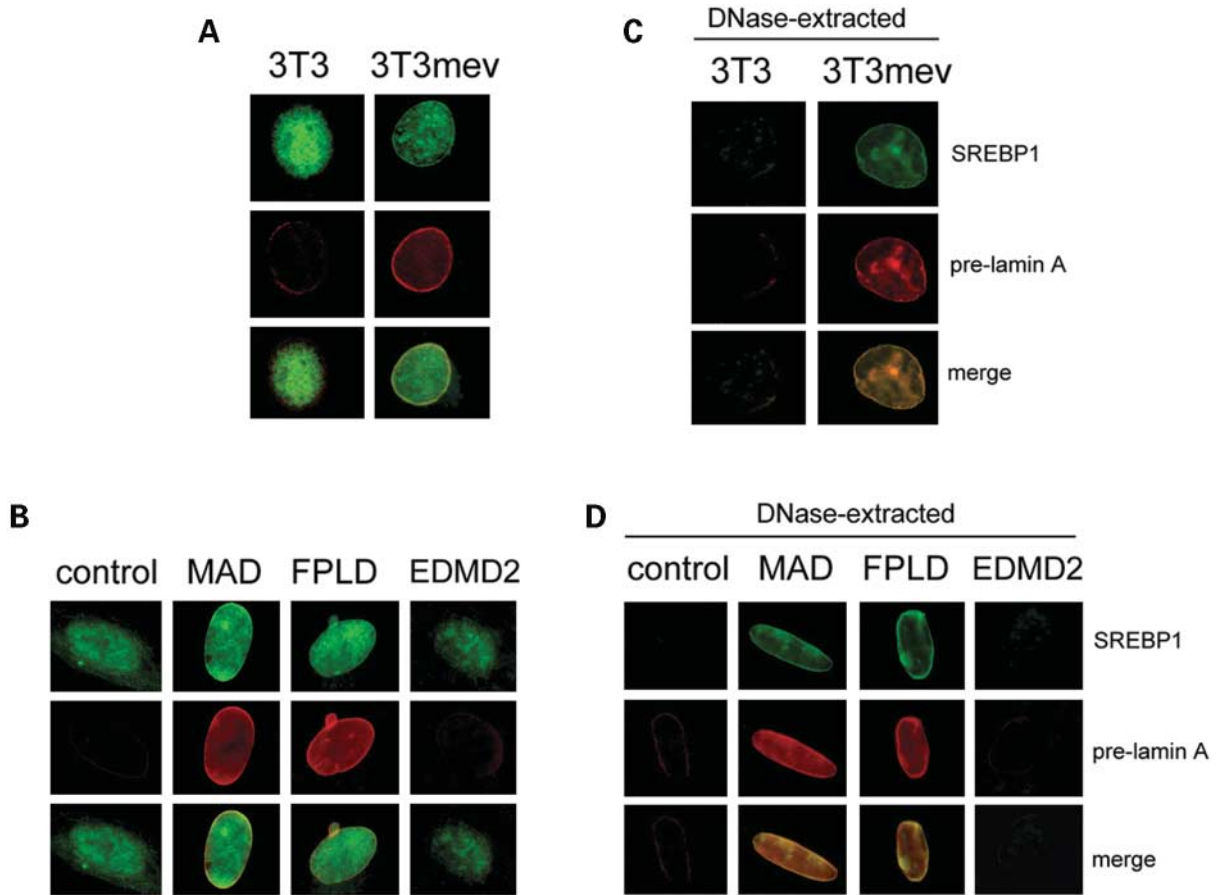Double immunofluorescence staining of SREBP1 and pre-lamin A was performed (Fig. 5). In untreated 3T3-L1

Figure 5. Localization of SREBP1 in the nuclei accumulating pre-lamin A. Cells were double-stained with anti-SREBP1 and anti-pre-lamin A antibody. SREBP1 is detected by FITC-conjugated secondary antibody (green) and pre-lamin A is detected by Cy-3 conjugated secondary antibody (red). **(A)** Localization of SREBP1 and pre-lamin A in untreated (3T3) or mevinolin-treated 3T3-L1 pre-adipocytes (3T3mev). **(B)** Double-immunofluorescence staining of SREBP1 and pre-lamin A in wild-type (control), MAD, FPLD and EDMD2 fibroblasts. **(C)** Localization of SREBP1 and pre-lamin A in untreated (3T3) or mevinolin-treated 3T3-L1 pre-adipocytes (3T3mev), following *in situ* extraction with DNase. DNase extraction of unfixed adherent cells was performed using 20 U/ml of DNase for 15 min at room temperature. Cells were double-stained as described earlier. **(D)** Double-immunofluorescence staining of SREBP1 and pre-lamin A in wild-type (control), MAD, FPLD and EDMD2 fibroblasts following DNase extraction. The merged images (merge) show yellow staining of the nuclear envelope in fibroblasts accumulating SREBP1 and pre-lamin A at the nuclear rim. The reported results are representative of three independent experiments.

pre-adipocytes (Fig. 5A), SREBP1 localized inside the nucleus (Fig. 5A). In mevinolin-treated 3T3-L1 pre-adipocytes, co-localization of SREBP1 and pre-lamin A at the nuclear rim was observed (Fig. 5A). In untreated nuclei from control fibroblasts (wild-type or EDMD2 fibroblasts), SREBP1 localized at the nuclear interior, whereas the transcription factor was also observed at the nuclear rim of MAD and FPLD fibroblasts (Fig. 5B). To support the evidence of SREBP1 retention in the nuclear insoluble fraction by pre-lamin A, *in situ*-DNase extraction was performed. Following DNase-digestion, SREBP1 was hardly detectable in the nuclei of 3T3-L1 cells which did not undergo mevinolin treatment, yet it was retained at the nuclear rim of mevinolin-treated pre-adipocytes, where it co-localized with pre-lamin A (Fig. 5C). SREBP1 labeling was almost undetectable in wild-type and EDMD2 fibroblasts following DNase treatment, whereas it was observed at the nuclear rim of DNase-extracted MAD and FPLD fibroblasts (Fig. 5D).

Pre-lamin A accumulation reduces PPARγ levels in 3T3-L1 nuclei and impairs adipocyte differentiation: rescue by TZD treatment

Since the transcription factor PPARγ is transcribed following SREBP1 activation in pre-adipocytes induced to differentiate (7,17), we checked PPARγ levels in differentiating 3T3-L1 cells accumulating pre-lamin A. To rule out the possibility that mevinolin could interfere with cholesterol synthesis by inhibiting HMG-CoA reductase, pre-lamin A accumulation was also obtained using the farnesyltransferase inhibitor FTI-277 or by transfecting cell cultures with an uncleavable pre-lamin A mutant (as described subsequently). PPARγ expression was strongly reduced in mevinolin-treated 3T3-L1 pre-adipocytes, as determined by western blot (Fig. 6A) and immunofluorescence analysis (Fig. 6B). Downregulation of PPARγ was also obtained using FTI-277 to accumulate pre-lamin A (data not shown). To support this observation, we transiently transfected 3T3-L1 pre-adipocytes with
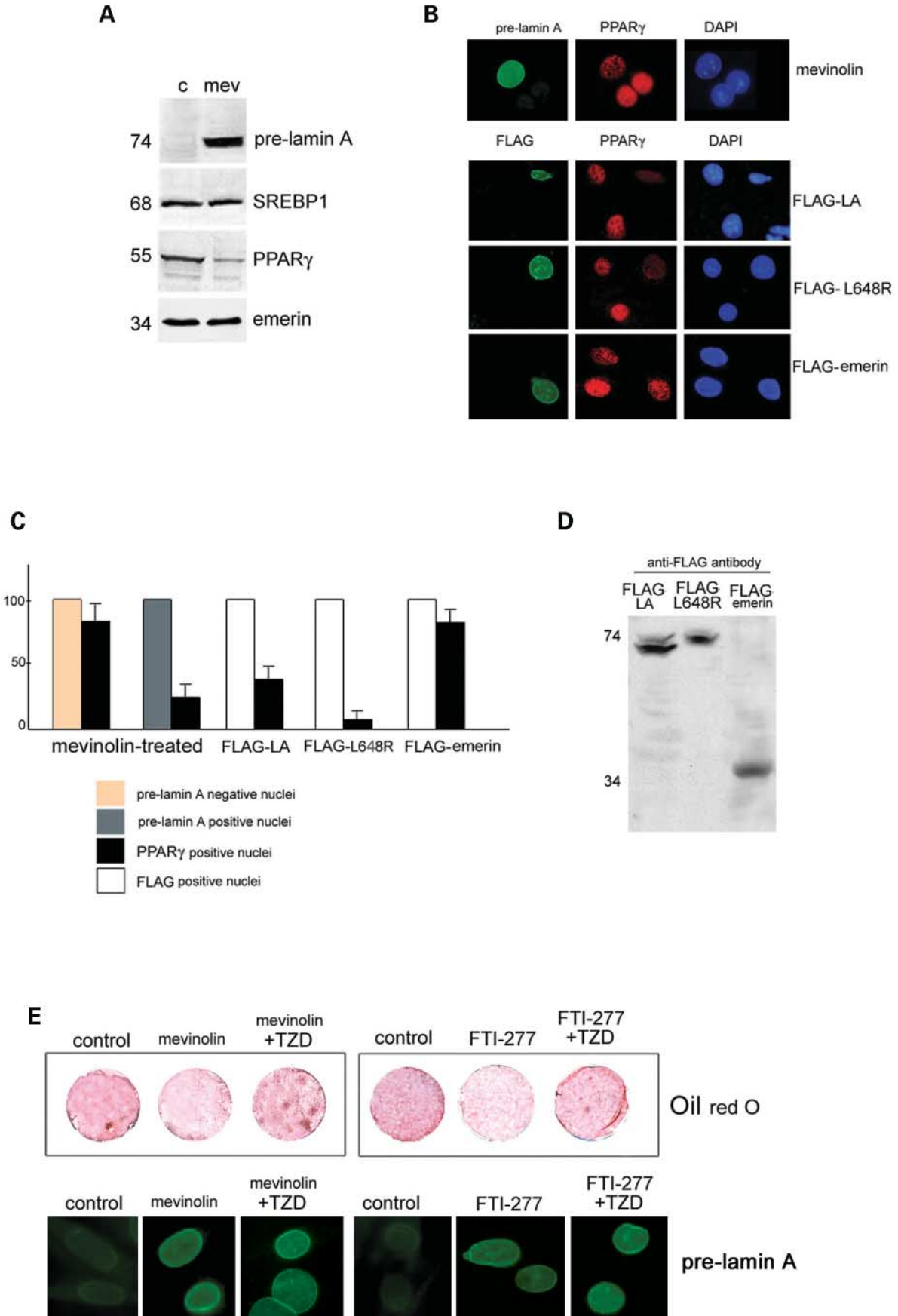
a FLAG-tagged lamin A construct overexpressing an unclea-vable L648R mutated pre-lamin A: PPARγ was downregu-lated in the nuclei accumulating FLAG–L648R pre-lamin A (Fig. 6B and C). Overexpression of wild-type FLAG–lamin A (FLAG–LA) was also effective in reducing PPARγ level (Fig. 6B and C), whereas PPARγ expression was not lowered in 3T3-L1 cells overexpressing the full-length emerin protein, here used as a control (Fig. 6B and C). Statisti-cal evaluation of these results showed that the percentage of PPARγ-labeled nuclei was significantly reduced in cells accumulating pre-lamin A (Fig. 6C). It should be noted that the 74 kDa pre-lamin A band only was detected in FLAG–L648R pre-lamin A-transfected cells by western immunoblot (Fig. 6D). On the other hand, accumulation of wild-type pre-lamin A along with mature lamin A occurred in pre-adipocytes overexpressing FLAG–LA (Fig. 6D).

Accumulation of pre-lamin A reduced adipocyte differen-tiation, as detected by oil red O staining of mevinolin- or FTI-277-treated 3T3-L1 cultures (Fig. 6E). However, 3T3-L1 cells treated with the PPARγ ligand TZD showed positive oil red O staining even after accumulation of pre-lamin A by mevinolin or by FTI-277 treatment (Fig. 6E), indicating the rescue of adipogenic differentiation.

DISCUSSION

The results reported here show that (i) accumulation of pre-lamin A specifically occurs in lipodystrophy-linked laminopa-thies, but not in EDMD2; (ii) *in vivo* binding of pre-lamin A to the adipocyte transcription factor SREBP1 does occur and it is detectable in cells accumulating pre-lamin A; (iii) pre-lamin A sequesters SREBP1 at the nuclear rim, thus reducing the pool of DNA-bound active transcription factor; (iv) retention of SREBP1 by pre-lamin A causes downregulation of PPARγ expression and hence reduces the rate of pre-adipocyte differ-entiation and (v) adipogenic differentiation of pre-adipocytes accumulating pre-lamin A may be rescued by PPARγ ago-nists. The overall evaluation of these results shows that a common pathogenic mechanism may be causative of different lipodystrophic phenotypes.

The proposed mechanism involves primarily in the accumu-lation of pre-lamin A and selective binding of the lamin A pre-cursor to the adipocyte transcription factor SREBP1. In MAD, FPLD and WS cells, we observed an accumulation of the lamin A precursor. Interestingly, the amount of pre-lamin A was not increased in EDMD2 fibroblast cell lines, indicating that impairment of lamin A precursor maturation is specifi-cally associated with lipodystrophy-linked lamin A mutations. However, the reason why lamin A processing is selectively affected by R482L, R527H and S143F *LMNA* mutations is not obvious. At present, we can rule out the possibility of altered interplay between pre-lamin A and farnesyltrans-ferases. In fact, mevinolin treatment was effective in increas-ing mutated pre-lamin A amount in MAD, FPLD and WS fibroblasts, suggesting that farnesylation of pre-lamin A is an ongoing mechanism in these cells (MAD being a recessive disease model, only expressing mutated lamin A). On the other hand, altered interaction of mutated pre-lamin A with ZPMSTE 24 endoprotease might affect protein processing. It is noteworthy that ZPMSTE 24 mutations lead to accumu-lation of pre-lamin A due to impaired cleavage of the farnesy-lated protein and cause MAD (13), HGPS (Markquardt, personal communication) and restrictive dermopathy (49) in humans and a MAD-resembling phenotype in mice (14,15).

We localized pre-lamin A-labeled intra-nuclear structures both in wild-type and in laminopathic cells accumulating the lamin A precursor. Such structures have been previously shown in wild-type cells induced to accumulate pre-lamin A (21,50). However, additional dominant negative effects of mutations appear to affect differently both number and shape of pre-lamin A-labeled structures in each laminopathic cell line. In the case of MAD and WS fibroblasts, pre-lamin-A-containing structures mostly protrude through the nuclear interior, as was also observed in control nuclei, whereas in R482L FPLD nuclei they are mostly localized at the nuclear lamina level. We recently noticed that the number of pre-lamin-A-labeled intra-nuclear structures and the level of lamin A precursor were significantly increased in older MAD patients, though carrying the same R527H *LMNA* mutation (data not shown). Noticeably, pre-lamin A-labeled structures may co-localize with emerin in wild-type and

Figure 6. Analysis of PPARγ expression and adipocyte differentiation in 3T3-L1 pre-adipocytes accumulating pre-lamin A. **(A)** 3T3-L1 pre-adipocytes were left untreated (c) or treated with mevinolin for 18 h (mev), thereafter allowed to differentiate for 4 days in differentiation medium. Nuclear lysates were obtained by hypotonic shock and shearing and subjected to electrophoresis and western blot analysis with anti-PPARγ and anti-pre-lamin A antibody. Immunoblotted mem-branes were stripped and re-probed with anti-SREBP1 and anti-emerin antibody. The 68 kDa SREBP1 band was detected in the nuclear fractions. Emerin was labeled as a loading control. Molecular weight markers are reported in kilodaltons. **(B)** 3T3-L1 pre-adipocytes grown on coverslips were treated with mevinolin or transfected with the indicated constructs and allowed to differentiate for 4 days. Double-immunofluorescence staining of pre-lamin A and PPARγ was per-formed in mevinolin-treated samples (mevinolin). Double-staining with anti-FLAG and anti-PPARγ antibodies was performed in FLAG–LA-transfected pre-adipocytes (FLAG–LA), L648R-lamin A-transfected adipocytes (FLAG–L648R) and emerin-transfected adipocytes (FLAG–emerin). DAPI staining allows visualization of all the nuclei. **(C)** Percentage of PPARγ-positive nuclei in 3T3-L1 pre-adipocytes subjected to mevinolin treatment (mevinolin-treated), over-expressing wild-type FLAG–LA, mutated L648R FLAG–LA (FLAG–L648R) or FLAG–emerin. One-thousand nuclei were counted per sample and data are reported as percentage of counted nuclei (±SEM) of three separate countings performed in independent experiments. **(D)** Western blot analysis of exogenous proteins expressed in 3T3-L1 cells (FLAG–LA, FLAG-tagged wild-type lamin A; FLAG–L648R, FLAG-tagged L648R-mutated lamin A; FLAG–emerin, FLAG-tagged wild-type emerin). Each construct was transfected in 3T3-L1 cells. Cellular lysates were subjected to western immunoblot using anti-FLAG anti-body. The 74 kDa band corresponds to FLAG–pre-lamin A, the 70 kDa band corresponds to FLAG–LA, the 34 kDa band corresponds to FLAG–emerin. **(E)** Pre-adipocyte differentiation was evaluated by oil red O staining of cultured 3T3-L1 cells on day 2 of differentiation. 3T3-L1 cultures were left untreated (control) or treated with mevinolin for 18 h or with FTI-277 for 24 h. Thereafter, cells were allowed to differentiate for 2 days either in the presence or in the absence of 10 μM TZD. An untreated culture (control) is shown on the left of each slide, a drug-treated culture (mevinolin or FTI-277) is shown in the middle and a culture treated with mevinolin or FTI-277 and then with TZD for further 48 h (mevinolin + TZD or FTI-277 + TZD) is shown on the right. Oil red O staining is increased in differentiated cells bearing fat deposits. Pre-lamin A staining of representative nuclei from each 3T3-L1 sample is shown in the lower row (pre-lamin A). Each of these pictures is representative of three independent experiments.

EDMD2 nuclei, but not in FPLD, MAD and WS nuclei, suggesting disease-specific changes of intermolecular interactions (42).

Because we had determined a link between pre-lamin A accumulation and *LMNA*-associated lipodystrophies, we decided to investigate whether pre-lamin A interacted with the transcription factor SREBP1, which mediates adipocyte differentiation (44). *In vitro* binding of SREBP1 to lamin A/C had been demonstrated by Lloyd *et al.* (34) and the site of interaction had been mapped between aminoacids 227 and 487 of SREBP1 N-terminus sequence (34). In the present study, we demonstrated for the first time *in vivo* binding of the lamin A precursor to SREBP1. As expected, the low-molecular-weight form of SREBP1 interacts with pre-lamin A, indicating involvement of the nuclear lamina protein in the localization of the active transcription factor. Interestingly, Lloyd *et al.* (34) performed a GST binding-assay with a lamin A peptide spanning aminoacids 389–664, which includes pre-lamin A C-terminal sequence. Thus, our results confirm that the whole unprocessed lamin A molecule is required for SREBP1 interaction *in vivo.* The previously suggested reduction of lamin A–SREBP1 binding affinity caused by R482 *LMNA* mutation (34) does not appear to affect *in vivo* interaction between pre-lamin A and SREBP1. This might be related to the increased availability of pre-lamin A in FPLD cells, which could overcome the reduced binding affinity caused by the mutation. In addition, we cannot rule out the possibility that a different aminoacid substitution (R482L instead of R482W) may differently affect protein interplay (42).

By treating pre-adipocytes with farnesylation inhibitors, we obtained a suitable cellular model that reproduced the situation of pre-lamin A accumulation in adipose tissue. This allowed us to investigate some biological mechanisms downstream of reduced pre-lamin A maturation.

We showed that the retention of active SREBP1 at the nuclear lamina occurs in pre-adipocytes accumulating pre-lamin A, as demonstrated by the significantly increased proportion of mature SREBP1 found in the nuclear insoluble fraction following DNase extraction. Immunofluorescence labeling allowed us to show co-localization of SREBP1 and pre-lamin A in the nuclei accumulating pre-lamin A. In fact, DNA-bound transcription factor disappears from control nuclei after the removal of DNA, whereas lamina-associated SREBP1 is still retained in the nuclei accumulating pre-lamin A and shows a typical nuclear rim staining. We suggest that the reduced rate of lamin A precursor processing allows detection of pre-lamin A-bound SREBP1, which is hardly detectable in control cell lines undergoing rapid pre-lamin A maturation.

It is noteworthy that SREBP1 nuclear translocation is impaired in *Lmna*-null mouse cardiomyocytes, but not in the adipose tissue from *Lmna* null mice (36), indicating that nuclear import of SREBP1 in adipocytes does not require *Lmna* products. These data and our present results support the view that SREBP1–pre-lamin A interplay has a physiological role in the negative regulation of SREBP1 nuclear translocation in adipose tissue, so that excess accumulation of pre-lamin A selectively sequesters SREBP1 at the adipocyte nuclear envelope. On the other hand, pre-lamin A might play a positive regulation role for SREBP1 nuclear import in other cell types such as cardiac myocytes (36). In agreement with this hypothesis, pre-lamin A–SREBP1 interplay, which is potentially disrupted by some *LMNA* mutations causing AD-EDMD (34), might be involved in the nuclear import of the transcription factor in skeletal muscle cells.

Retention of SREBP1 at the nuclear rim was previously reported in 3T3-F442A pre-adipocytes treated with Indinavir, a drug employed in HAART and causing lipodystrophy as a side-effect (7). Under these experimental conditions, 3T3-F442A fibroblasts show increased pre-lamin A level and reduced PPARγ expression (7). These and our results strongly suggest that retention of SREBP1 at the nuclear rim of lipodystrophy cells is associated with the presence of increased pre-lamin A level, irrespective of the occurrence of *LMNA* mutations. In fact, the identification of a selective and stable interplay between pre-lamin A and SREBP1 helps to explain the pathophysiology of both acquired and inherited lipodystrophy, the latter due to either lamin A/C or ZMPSTE 24 mutations. Moreover, it is noteworthy that farnesyltransferase inhibitors (causing pre-lamin A accumulation) have been previously reported to impair adipocyte differentiation (51,52). Our results help in explaining the biological mechanism underlying this effect.

A key event of adipocyte differentiation is the induction of the transcription factor PPARγ which is triggered by SREBP1 (48). Downregulation of PPARγ expression was obtained in pre-adipocytes accumulating the lamin A precursor either by mevinolin treatment or by overexpressing uncleavable pre-lamin A. Uncleavable mutants of lamin A have been shown to assemble and localize at the nuclear envelope with kinetics comparable with that of wild-type protein (53). The L648R-lamin A mutant did in fact localize at the nuclear envelope, where it could potentially bind SREBP1, as observed for de-farnesylated pre-lamin A. Interestingly, a reduced PPARγ level was also observed in adipocytes accumulating wild-type FLAG–pre-lamin A. In the latter case, the increase of pre-lamin A level was directly attributable to overexpression of the exogenous protein. These results support the view that excess accumulation of pre-lamin A is sufficient to sequester an amount of SREBP1, even in the presence of mature lamin A. Thus, PPARγ induction, a key step of adipocyte differentiation, may be altered in laminopathies featuring lipodystrophy, as already proposed for acquired lipodystrophies (7,16).

In fact, adipocyte differentiation was impaired by pre-lamin A accumulation, as determined by oil red O staining of mevinolin- or FTI-277-treated pre-adipocyte cultures. Given that FTI-277 selectively affects pre-lamin A processing without any interference with ras protein farnesylation or with cholesterol synthesis (54), we conclude that reduced adipocyte differentiation is a direct effect of pre-lamin A accumulation. It should be noted that highly differentiated cultures were not affected by drug treatment (data not shown), in agreement with the evidence that an early event in the adipocyte differentiation pathway, such as PPARγ activation, is affected by pre-lamin A.

PPARγ expression has been reported to be regulated dependent on the body district (55). This important observation suggests that pre-lamin A accumulation may elicit different

effects in different fat depots depending on the extent of PPARγ activation required in that particular area. This could, in part, explain the selective involvement of some but not all adipose tissue districts in partial lipodystrophies.

Treatment of 3T3-L1 cells accumulating pre-lamin A with the PPARγ ligand TZD elicited rescue of the adipogenic program. The latter finding gives an important insight into possible therapeutic approaches to lipodystrophy, which have been already reported to elicit some promising effects (56).

As MAD is a recessive disease, one would expect pre-lamin A accumulation even in the heterozygous state, i.e. in a percentage of cells from parents of affected individuals bearing one mutated allele (3). We did not observe a significant increase of pre-lamin A amount in those cells. However, this study deserves further deepening, since we found that overexpression of R527H-mutated lamin A in transfected cells causes accumulation of mutated pre-lamin A (but not endogenous pre-lamin A) (data not shown). On the other hand, MAD phenotype is not observed in heterozygous individuals, strongly supporting the view that a threshold pre-lamin A level is required to activate the pathogenic mechanism. Regarding the pathophysiology of MAD and WS, two main questions need further investigation. The first is the effect elicited by the accumulation of lamin A precursor protein in osteoblasts. In fact, bone resorption of the extremities is a specific feature of MAD phenotype (3) and osteoporosis is also observed in WS patients (11) (though it might be related to the aging process featuring this disease). We are now addressing this problem by evaluating the effect of high pre-lamin A level in pre-osteocyte differentiation or survival. The other open question is the pathogenetic mechanism leading to a premature aging phenotype in MAD patients and mostly in WS patients. We suggest that this phenotype could be dependent both on an anomalous amount of pre-lamin A and on altered interaction between mutated lamin A/C and its nuclear binding partners.

MATERIALS AND METHODS

Cell culture and differentiation

Skin biopsies were obtained from a MAD patient carrying an R527H lamin A/C mutation (3), an FPLD patient carrying an R482L lamin A/C mutation (42), an atypical WS patient carrying an S143F *LMNA* mutation, an EDMD2 patient carrying R401C *LMNA* mutation and from unaffected controls following their written consent. Fibroblast cultures were established and cultured in Dulbecco's modified Eagle's medium (DMEM) supplemented with 10% fetal calf serum (FCS) and antibiotics. Cells at passages 10–15 were employed. 3T3-L1 pre-adipocytes were obtained from the European Collection of Cell Cultures and cultured in DMEM plus 10% FCS. Pre-adipocytes approaching confluence were induced to differentiate by incubation for 2 days in a differentiation medium containing DMEM plus 10% FCS, 5 μg/ml insulin, 0.25 μM dexamethasone and 0.1 mM 3-isobutyl-1-methylxanthine. Thereafter, incubation was performed for an additional 2 days in the same medium excluding dexamethasone and 3-isobutyl-1-methylxanthine. Cells were

maintained for 8–10 days in DMEM with 10% FCS to attain maximal differentiation (57).

Transfection of pre-adipocyte cultures

A full-length rat lamin A cDNA encoding for pre-lamin A was expressed from the CMV promoter and tagged at the 5′ end with a sequence coding for FLAG epitope (FLAG–LA) (58). The L648R point mutation was introduced into the full-length rat lamin A cDNA using the QuikChange site-directed mutagenesis kit (Stratagene, La Jolla, CA, USA). This mutation impairs cleavage of pre-lamin A by ZMPSTE24 endoprotease and causes accumulation of farnesylated pre-lamin A (12). FLAG–LA or L648R–FLAG-lamin A was transfected in 3T3-L1 pre-adipocytes at day 0 of differentiation. A FLAG-tagged wild-type emerin construct was used to transfect pre-adipocytes as a control. Transfection of 3T3-L1 pre-adipocytes was performed using FuGene 6 reagent according to the manufacturer's instructions. Cells were fixed at day 4 of differentiation.

Drug treatments

Pre-lamin A accumulation in human fibroblasts and 3T3-L1 adipocytes was induced by inhibition of isoprenoid synthesis with 25 μM Mevinolin (Sigma) for 18 h (21). This drug subtracts the substrate of farnesyltransferases, thus impairing pre-lamin A farnesylation which is required for further protein processing (59). Alternatively, pre-lamin A farnesylation was inhibited using the peptidomimetic drug FTI-277 (Calbiochem), which selectively impairs pre-lamin A farnesylation, at the dosage used (20 μM for 24 h) (54). Treatment with TZD (Sigma) was performed according to the published protocols to trigger PPARγ activation (16). Briefly, 3T3-L1 pre-adipocytes were induced to accumulate pre-lamin A by 18 h mevinolin treatment or by 24 h FTI-277 treatment. Thereafter, cells were transferred in culture medium, containing or not 10 μM TZD, and incubated for 48 h. Incubation was stopped by formalin fixation, as described subsequently.

Sub-cellular fractioning and DNase treatment

Sub-cellular fractions were obtained as previously described (26). Briefly, the cell pellet was resuspended in a lysis buffer containing 10 mM Tris, pH 7.8, 1% NP-40, 10 mM 2-mercaptoethanol and protease inhibitors. Separation of nuclei was obtained by hypotonic shock and shearing; nuclei were obtained as pellet by a 300g centrifugation at 4°C. Other samples were treated by the same procedure and employed to obtain the cytoplasmic fraction as supernatant. Cytoplasmic fractions were clarified by centrifugation at 600g. DNase extraction of nuclei was performed according to published protocols (42) except that 100 U/ml of DNase was applied for 30 min. The insoluble nuclear fraction (N^P in Fig. 4), containing nuclear matrix constituents, was obtained as pellet. Each fraction was then resuspended in loading buffer, subjected to sodium dodecyl sulphate–polyacrylamide gel electrophoresis (SDS–PAGE) and western blot analysis.

In situ DNase extraction was performed as follows. Unfixed cell cultures were washed in phosphate-buffered saline (PBS), treated with a buffer containing 10 mM Tris–HCl (pH 7.4), 150 mM NaCl, 5 mM MgCl$_2$, 1% NP-40, 1 mM phenylmethylsulfonyl fluoride (PMSF), 10 µg/ml leupeptin and aprotinin for 15 min at room temperature. Detergent-treated cells were washed twice in the absence of NP-40 and subjected to DNase treatment (20 U/ml for 15 min at room temperature). Samples were fixed with 4% paraformaldehyde and processed for immunofluorescence labeling.

Antibodies

The antibodies employed for western blot analysis or immunofluorescence labeling were as follow: anti-lamin A/C, monoclonal (Novocastra Laboratories, NCL-LAM-A/C); anti-lamin A/C, goat polyclonal, (Santa Cruz, sc-6215); anti-pre-lamin A, goat polyclonal (Santa Cruz, sc-6214) (15); anti-SREBP1, rabbit polyclonal (Santa Cruz, sc-8984); anti-emerin, mouse monoclonal (Novocastra Laboratories, NCL-emerin); anti-PPARγ, mouse monoclonal (Santa Cruz, sc-7273); anti-actin, goat polyclonal (Santa Cruz, sc-1616) and anti-FLAG, rabbit polyclonal (Sigma, F-7425).

Western blot and immunoprecipitation

Western blot analysis of cellular lysates from human fibrobasts and 3T3-L1 pre-adipocytes was done as follows. Cells were lysed in buffer containing 1% NP-40, 0.25% sodium deoxycholate, 150 mM NaCl, 1 mM EGTA, 1 mM PMSF, 1 mM NaF, 1 µM aprotinin, leupeptin and pepstatin. Proteins were loaded in Laemmli sample buffer and subjected to SDS–PAGE followed by immunochemical reactions. For immunoprecipitation analysis, human fibroblasts and 3T3-L1 pre-adipocytes were treated with a buffer containing 50 mM HEPES–HCl pH 7.4, 100 mM NaCl, 1% NP-40, 1 mM PMSF, 1 mM dithiothreitol, 1.5 mM MgCl$_2$, 10 µM of each leupeptin, pepstatin, aprotinin for 10 min at 4°C. After sonication, cell extracts were clarified by 12 000g centrifugation at 4°C. Protein A/G–Sepharose beads were incubated with anti-SREBP1 or with anti-pre-lamin A antibodies for 14 h at 4°C and unbound antibodies were removed by centrifugation. Cellular extracts were incubated with antibody-coupled Sepharose beads for 3 h at 4°C. Immunoprecipitated complexes were diluted in Laemmli buffer, subjected to SDS–PAGE (6–20%) and transferred to nitrocellulose membrane. Membranes were saturated with 5% dried skimmed milk–4% bovine serum albumin (BSA) and incubation with primary antibodies was performed for 1 h at room temperature. Immunoblotted bands were revealed by the Amersham ECL detection system. Densitometry of immunoblotted bands was performed by a Biorad GS-800 calibrated densitometer. Statistical analysis was performed by Student's t-test.

Immunofluorescence

Human fibroblasts and 3T3-L1 pre-adipocytes grown on coverslips were fixed in methanol at 20°C. *In situ* DNase extracted samples were fixed by 4% paraformaldehyde. Samples were incubated with PBS containing 4% BSA to saturate non-specific binding. Primary antibodies were applied overnight at 4°C, secondary antibodies were applied for 1 h at room temperature. Slides were mounted with an anti-fade reagent in glycerol and observed with a Nikon E 600 fluorescence microscope equipped with a digital camera. Pictures were elaborated with Photoshop-6 software.

Oil red O staining

Oil red O staining of cultured 3T3-L1 pre-adipocytes was performed to stain lipid droplets. Cells were fixed for 1 h at room temperature with 10% formalin in isotonic buffer, washed three times with distilled water, and then stained with 0.6% (wt/vol) oil red O solution (60% isopropanol, 40% water) for 1 h at 22°C. After washing three times with distilled water, the cells were examined under a microscope (16).

REFERENCES

1. Hegele, R.A. (2003) Monogenic forms of insulin resistance: apertures that expose the common metabolic syndrome. *Trends Endocrinol. Metab.*, **14**, 371–377.
2. Shacketon, S., Lloyd, D.J., Jackson, SN., Evans, R., Niermeijer, M.F., Singh, B.M., Schmidt, H., Brabant, G., Kumar, S. *et al.* (2000) LMNA, encoding lamin A/C, is mutated in partial lipodystrophy. *Nat. Genet.*, **24**, 153–156.
3. Novelli, G., Muchir, A., Sangiuolo, F., Helbling-Leclerc, A., D'Apice, M.R., Massart, C., Capon, F., Sbraccia, P., Federici, M., Lauro, R. *et al.* (2002) Mandibuloacral dysplasia is caused by a mutation in LMNA-encoding lamin A/C. *Am. J. Hum. Genet.*, **71**, 426–431.
4. Bhayana, S., Siu, V.M., Joubert, G.I., Clarson, C.L., Cao, H. and Hegele, R.A. (2002) Cardiomyopathy in congenital complete lipodystrophy. *Clin. Genet.*, **61**, 283–287.
5. Magre, J.J., Delepine, M., Khallouf, E., Gedde-Dahl, T., Jr, van Maldergem, L., Sobel, E., Papp, J., Meier, M., Megarbane, A., Bachy, A. *et al.* (2001) Identification of the gene altered in Berardinelli–Seip congenital lipodystrophy on chromosome 11q13. *Nat. Genet.*, **28**, 365–370.
6. Hegele, R.A., Cao, H., Frankowski, C., Mathews, S.T. and Leff, T. (2002) PPARG F388L, a transactivation-deficient mutant, in familial partial lipodystrophy. *Diabetes*, **51**, 3586–3590.
7. Caron, M., Auclair, M., Sterlingot, H., Kornprobst, M. and Capeau, J. (2003) Some HIV protease inhibitors alter lamin A/C maturation and stability, SREBP-1 nuclear localization and adipocyte differentiation. *AIDS*, **17**, 2437–2444.

8. de Sandre-Giovannoli, A., Bernard, R., Cau, P., Navarro, C., Amiel, J., Boccaccio, I., Lyonnet, S., Stewart, C.L., Munnich, A., Le Merrer, M. *et al* (2003) Lamin a truncation in Hutchinson–Gilford progeria. *Science*, **300**, 2055.

9. Eriksson, M., Brown, W.T., Gordon, L.B., Glynn, M.W., Singer, J., Scott, L., Erdos, M.R., Robbins, C.M., Moses, T.Y., Berglund, P. *et al.* (2003) Recurrent *de novo* point mutations in lamin A cause Hutchinson–Gilford progeria syndrome. *Nature*, **423**, 293–298.

10. Cao, H. and Hegele, R.A. (2003) LMNA is mutated in Hutchinson–Gilford progeria (MIM 176670) but not in Wiedemann–Rautenstrauch progeroid syndrome (MIM 264090). *J. Hum. Genet.*, **48**, 271–274.

11. Chen, L., Lee, L., Kudlow, B.A., Dos Santos, H.G., Sletvold, O., Shafeghati, Y., Botha, E.G., Garg, A., Hanson, N.B., Martin, G.M. *et al.* (2003) LMNA mutations in atypical Werner's syndrome. *Lancet*, **362**, 440–445.

12. Corrigan, D.P., Kuszczak, D., Rusinol, A.E., Thewke, D.P., Hrycyna, C.A., Michaelis, S., Sinensky, M.S. (2005) Prelamin A endoproteolytic processing *in vitro* by recombinant Zmpste24. *Biochem. J.*, **387**, 129–138.

13. Agarwal, A.K., Fryns, J.P., Auchus, R.J. and Garg, A. (2003) Zinc metalloproteinase, ZMPSTE24, is mutated in mandibuloacral dysplasia. *Hum. Mol. Genet.*, **12**, 1995–2001.

14. Bergo, M.O., Gavino, B., Ross, J., Schmidt, W.K., Hong, C., Kendall, L.V., Mohr, A., Meta, M., Genant, H., Jiang, Y. *et al.* (2002) Zmpste24 deficiency in mice causes spontaneous bone fractures, muscle weakness, and a prelamin A processing defect. *Proc. Natl Acad. Sci. USA*, **99**, 13049–13054.

15. Pendas, A.M., Zhou, Z., Cadinanos, J., Freije, J.M., Wang, J., Hultenby, K., Astudillo, A., Wernerson, A., Rodriguez, F., Tryggvason, K. *et al* (2002) Defective prelamin A processing and muscular and adipocyte alterations in Zmpste24 metalloproteinase-deficient mice. *Nat. Genet.*, **31**, 94–99.

16. Caron, M., Auclair, M., Vigouroux, C., Glorian, M., Forest, C. and Capeau, J. (2001) The HIV protease inhibitor indinavir impairs sterol regulatory element-binding protein-1 intranuclear localization, inhibits preadipocyte differentiation, and induces insulin resistance. *Diabetes*, **50**, 1378–1388.

17. Spiegelman, B.M. (1998) PPAR-gamma: adipogenic regulator and thiazolidinedione receptor. *Diabetes*, **47**, 507–514.

18. Agarwal, A.K. and Garg, A. (2002) A novel heterozygous mutation in peroxisome proliferator-activated receptor-gamma gene in a patient with familial partial lipodystrophy. *J. Clin. Endocrinol. Metab.*, **87**, 408–411.

19. Al-Shali, K., Cao, H., Knoers, N., Hermus, A.R., Tack, C.J., Hegele, R.A. (2004) A single-base mutation in the peroxisome proliferator-activated receptor {gamma} promoter associated with altered *in vitro* expression and partial lipodystrophy. *J. Clin. Endocrinol. Metab.*, **89**, 5655–5660.

20. Zastrow, M.S., Vlcek, S. and Wilson, K.L. (2004) Proteins that bind A-type lamins: integrating isolated clues. *J. Cell. Sci.*, **117**, 979–987.

21. Sasseville, A.M. and Raymond, Y. (1995) Lamin A precursor is localized to intranuclear foci. *J. Cell. Sci.*, **108**, 273–285.

22. Stuurman, N., Heins, S. and Aebi, U. (1998) Nuclear lamins: their structure, assembly, and interactions. *J. Struct. Biol.*, **122**, 42–66.

23. Sakaki, M., Koike, H., Takahashi, N., Sasagawa, N., Tomioka, S., Arahata, K. and Ishiura, S. (2001) Interaction between emerin and nuclear lamins. *J. Biochem.*, **129**, 321–327.

24. Markiewicz, E., Dechat, T., Foisner, R., Quinlan, R.A. and Hutchison, C.J. (2002) Lamin A/C binding protein LAP2alpha is required for nuclear anchorage of retinoblastoma protein. *Mol. Biol. Cell*, **13**, 4401–4413.

25. Sasseville, A.M. and Langelier, Y. (1998) *In vitro* interaction of the carboxy-terminal domain of lamin A with actin. *FEBS Lett.*, **425**, 485–489.

26. Lattanzi, G., Cenni, V., Marmiroli, S., Capanni, C., Mattioli, E., Merlini, L., Squarzoni, S. and Maraldi, N.M. (2003) Association of emerin with nuclear and cytoplasmic actin is regulated in differentiating myoblasts. *Biochem. Biophys. Res. Commun.*, **303**, 764–770.

27. Mancini, M.A., Shan, B., Nickerson, J.A., Penman, S. and Lee, W.H. (1994) The retinoblastoma gene product is a cell cycle-dependent, nuclear matrix-associated protein. *Proc. Natl Acad. Sci. USA*, **91**, 418–422.

28. Novelli, G. and D'Apice, M.R. (2003) The strange case of the 'lumper' lamin A/C gene and human premature ageing. *Trends Mol. Med.*, **9**, 370–375.

29. Bonne, G., Raffaele-Di Barletta, M., Varnous, S., Becane, H.M., Hammouda, E.H., Merlini, L., Muntoni, F., Greenberg, C.R., Gary, F., Urtizberea, J.A. *et al.* (1999) Mutations in the gene encoding lamin A/C cause autosomal dominant Emery–Dreifuss muscular dystrophy. *Nat. Genet.*, **21**, 285–288.

30. Muchir, A., Bonne, G., van der Kooi, A.J., van Meegen, M., Baas, F., Bolhuis, P.A., de Visser, M. and Schwartz, K. (2000) Identification of mutations in the gene encoding lamins A/C in autosomal dominant limb girdle muscular dystrophy with atrioventricular conduction disturbances (LGMD1B). *Hum. Mol. Genet.*, **9**, 1453–1459.

31. Fatkin, D., MacRae, C., Sasaki, T., Wolff, M.R., Porcu, M., Frenneaux, M., Atherton, J., Vidaillet, H.J., Jr, Spudich, S., de Girolami, U. *et al.* (1999) Missense mutations in the rod domain of the lamin A/C gene as causes of dilated cardiomyopathy and conduction-system disease. *N. Engl. J. Med.*, **341**, 1715–1724.

32. de Sandre-Giovannoli, A., Chaouch, M., Kozlov, S., Vallat, J.M., Tazir, M., Kassouri, N., Szepetowski, P., Hammadouche, T., Vandenberghe, A., Stewart, C.L. *et al.* (2002) Homozygous defects in LMNA, encoding lamin A/C nuclear-envelope proteins, cause autosomal recessive axonal neuropathy in human (Charcot–Marie tooth disorder type 2) and mouse. *Am. J. Hum. Genet.*, **70**, 726–736.

33. Sullivan, T., Escalante-Alcalde, D., Bhatt, H., Anver, M., Bhat, N., Nagashima, K., Stewart, C.L. and Burke, B. (1999) Loss of A-type lamin expression compromises nuclear envelope integrity leading to muscular dystrophy. *J. Cell. Biol.*, **147**, 913–920.

34. Lloyd, D.J., Trembath, R.C. and Shackleton S. (2002) A novel interaction between lamin A and SREBP1: implications for partial lipodystrophy and other laminopathies. *Hum. Mol. Genet.*, **11**, 769–777.

35. Krimm, I., Ostlund, C., Gilquin, B., Couprie, J., Hossenlopp, P., Mornon, J.P., Bonne, G., Courvalin, J.C., Worman, H.J. and Zinn-Justin, S. (2002) The Ig-like structure of the C-terminal domain of lamin A/C, mutated in muscular dystrophies, cardiomyopathy, and partial lipodystrophy. *Structure*, **10**, 811–823.

36. Nikolova, V., Leimena, C., McMahon, A.C., Tan, J.C., Chandar, S., Jogia, D., Kesteven, S.H., Michalicek, J., Otway, R., Verheyen, F. *et al.* (2004) Defects in nuclear structure and function promote dilated cardiomyopathy in lamin A/C-deficient mice. *J. Clin. Invest.*, **113**, 357–369.

37. Lammerding, J., Schulze, P.C., Takahashi, T., Kozlov, S., Sullivan, T., Kamm, R.D., Stewart, C.L. and Lee, R.T. (2004) Lamin A/C deficiency causes defective nuclear mechanics and mechanotransduction. *J. Clin. Invest.*, **113**, 370–378.

38. Sabatelli, P., Lattanzi, G., Ognibene, A., Columbaro, M., Capanni, C., Merlini, L. Maraldi, N.M. and Squarzoni, S. (2001) Nuclear alterations in autosomal-dominant Emery–Dreifuss muscular dystrophy. *Muscle Nerve*, **24**, 826–829.

39. Maraldi, N.M., Lattanzi, G., Marmiroli, S., Squarzoni, S. and Manzoli, F.A. (2004) New roles for lamins, nuclear envelope proteins and actin in the nucleus. *Adv. Enzyme Regul.*, **44**, 155–172.

40. Stierle, V., Couprie, J., Ostlund, C., Krimm, I., Zinn-Justin, S., Hossenlopp, P., Worman, H.J., Courvalin, J.C. and Duband-Goulet, I. (2003) The carboxyl-terminal region common to lamins A and C contains a DNA binding domain. *Biochemistry*, **42**, 4819–4828.

41. Muchir, A., van Engelen, B.G., Lammens, M., Mislow, J.M., McNally, E., Schwartz, K. and Bonne, G. (2003) Nuclear envelope alterations in fibroblasts from LGMD1B patients carrying nonsense Y259X heterozygous or homozygous mutation in lamin A/C gene. *Exp. Cell Res.*, **291**, 352–362.

42. Capanni, C., Cenni, V., Mattioli, E., Sabatelli, P., Ognibene, A., Columbaro, M., Parnaik, V.K., Wehnert, M., Maraldi, N.M., Squarzoni, S. *et al.* (2003) Failure of lamin A/C to functionally assemble in R482L mutated familial partial lipodystrophy fibroblasts: altered intermolecular interaction with emerin and implications for gene transcription. *Exp. Cell Res.*, **291**, 122–134.

43. Tontonoz, P., Kim, J.B., Graves, R.A. and Spiegelman, B.M. (1993) ADD1: a novel helix-loop-helix transcription factor associated with adipocyte determination and differentiation. *Mol. Cell. Biol.*, **13**, 4753–4759.

44. Kim, J.B. and Spiegelman, B.M. (1996) ADD1/SREBP1 promotes adipocyte differentiation and gene expression linked to fatty acid metabolism. *Genes Dev.*, **10**, 1096–1107.

45. Ericsson, J., Jackson, S.M., Kim, J.B., Spiegelman, B.M. and Edwards, P.A. (1997) Identification of glycerol-3-phosphate acyltransferase as an adipocyte determination and differentiation factor 1- and sterol regulatory element-binding protein-responsive gene. *J. Biol. Chem.*, **272**, 7298–7305.

46. Kim, J.B., Wright, H.M., Wright, M. and Spiegelman, B.M. (1998) ADD1/SREBP1 activates PPARgamma through the production of endogenous ligand. *Proc. Natl Acad. Sci. USA*, **95**, 4333–4337.

47. Wang, X., Sato, R., Brown, M.S., Hua, X. and Goldstein, J.L. (1994) SREBP-1, a membrane-bound transcription factor released by sterol-regulated proteolysis. *Cell*, **77**, 53–62.

48. Hegele, R.A. (2001) Molecular basis of partial lipodystrophy and prospects for therapy. *Trends Mol. Med.*, **7**, 121–126.

49. Navarro, C.L., de Sandre-Giovannoli, A., Bernard, R., Boccaccio, I., Boyer, A., Genevieve, D., Hadj-Rabia, S., Gaudy-Marqueste, C., Smitt, H.S., Vabres, P., Faivre, L. *et al.* (2004) Lamin A and ZMPSTE24 (FACE-1) defects cause nuclear disorganization and identify restrictive dermopathy as a lethal neonatal laminopathy. *Hum. Mol. Genet.*, **13**, 2493–2503.

50. Maraldi, N.M., Squarzoni, S., Sabatelli, P., Capanni, C., Mattioli, E., Ognibene, A. and Lattanzi, G. (2005) Laminopathies: involvement of structural nuclear proteins in the pathogenesis of an increasing number of human diseases. *J. Cell Physiol.*, **203**, 319–327.

51. Nishio, E., Tomiyama, K., Nakata, H. and Watanabe, Y. (1996) 3-Hydroxy-3-methylglutaryl coenzyme A reductase inhibitor impairs cell differentiation in cultured adipogenic cells (3T3-L1). *Eur. J. Pharmacol.*, **301**, 203–206.

52. Solomon, C.S., Leitner, J.W. and Goalstone, M.L. (2003) Dominant negative alpha-subunit of farnesyl- and geranylgeranyl-transferase I inhibits insulin-induced differentiation of 3T3-L1 pre-adipocytes. *Int. J. Obes. Relat. Metab. Disord.*, **27**, 40–47.

53. Hennekes, H. and Nigg, E.A. (1994) The role of isoprenylation in membrane attachment of nuclear lamins. A single point mutation prevents proteolytic cleavage of the lamin A precursor and confers membrane binding properties. *J. Cell Sci.*, **107**, 1019–1029.

54. Adjei, A.A., Davis, J.N., Erlichman, C., Svingen, P.A. and Kaufmann, S.H. (2000) Comparison of potential markers of farnesyltransferase inhibition. *Clin. Cancer Res.*, **6**, 2318–2325.

55. Sewter, C.P., Blows, F., Vidal-Puig, A. and O'Rahilly, S. (2002) Regional differences in the response of human pre-adipocytes to PPARgamma and RXRalpha agonists. *Diabetes*, **51**, 718–723.

56. Owen, K.R., Donohoe, M., Ellard, S. and Hattersley, A.T. (2003) Response to treatment with rosiglitazone in familial partial lipodystrophy due to a mutation in the LMNA gene. *Diabet. Med.*, **20**, 823–827.

57. Parpal, S., Karlsson, M., Thorn, H. and Stralfors, P. (2001) Cholesterol depletion disrupts caveolae and insulin receptor signaling for metabolic control via insulin receptor substrate-1, but not for mitogen-activated protein kinase control. *J. Biol. Chem.*, **276**, 9670–9678.

58. Kumaran, R.I., Muralikrishna, B. and Parnaik, V.K. (2002) Lamin A/C speckles mediate spatial organization of splicing factor compartments and RNA-polymerase II transcription. *J. Cell Biol.*, **159**, 783–793.

59. Sinensky, M., Beck, L.A., Leonard, S. and Evans, R. (1990) Differential inhibitory effects of lovastatin on protein isoprenylation and sterol synthesis. *J. Biol. Chem.*, **265**, 19937–19941.